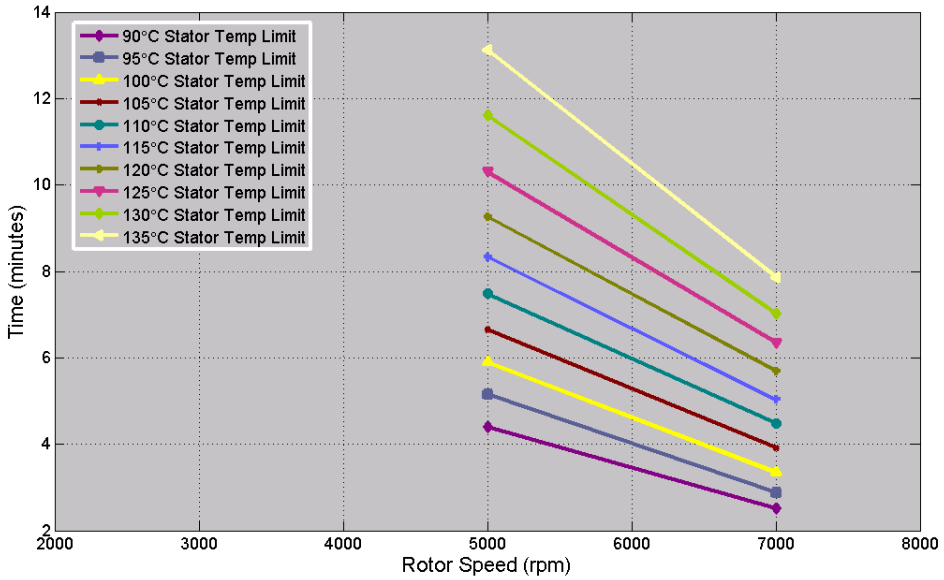

Fig. 3.33. Camry 50 kW continuous duration vs. speed with 35ºC coolant.

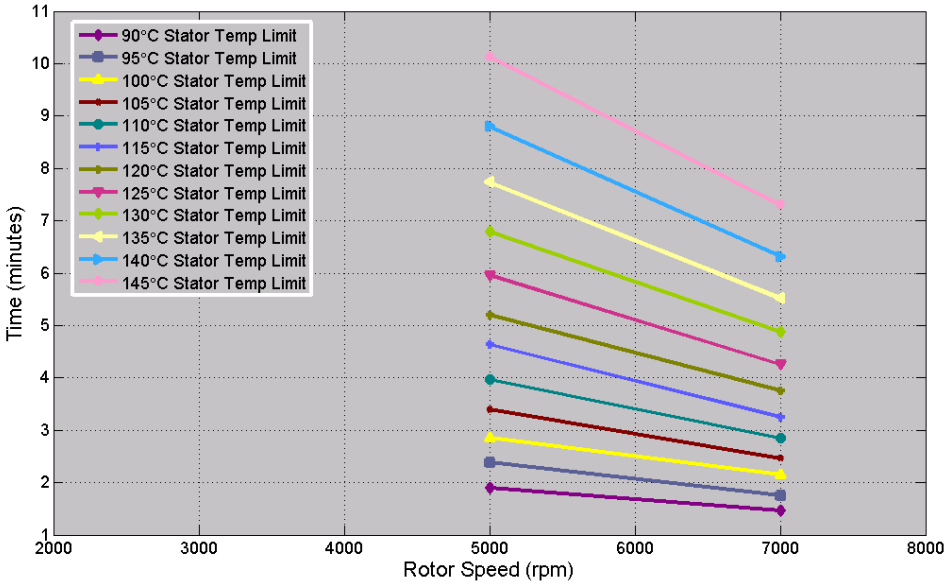

Fig. 3.34. Camry 50 kW continuous duration vs. speed with 65ºC coolant.

The previous graphs provided a clear indication of the influence of speed and coolant temperature upon duration capabilities. To provide a more clear assessment of the impact of stator temperature limitations and coolant temperature upon duration capability, duration time is plotted versus the stator temperature limit in Fig. 3.35 for operations at 3000 rpm. Each trace represents a particular power level and coolant temperature combination. In studying the figure, it is evident that coolant temperature does not affect operation duration greatly at 33.5 kW, yet coolant temperature greatly affects operation duration at a power level of 25 kW.

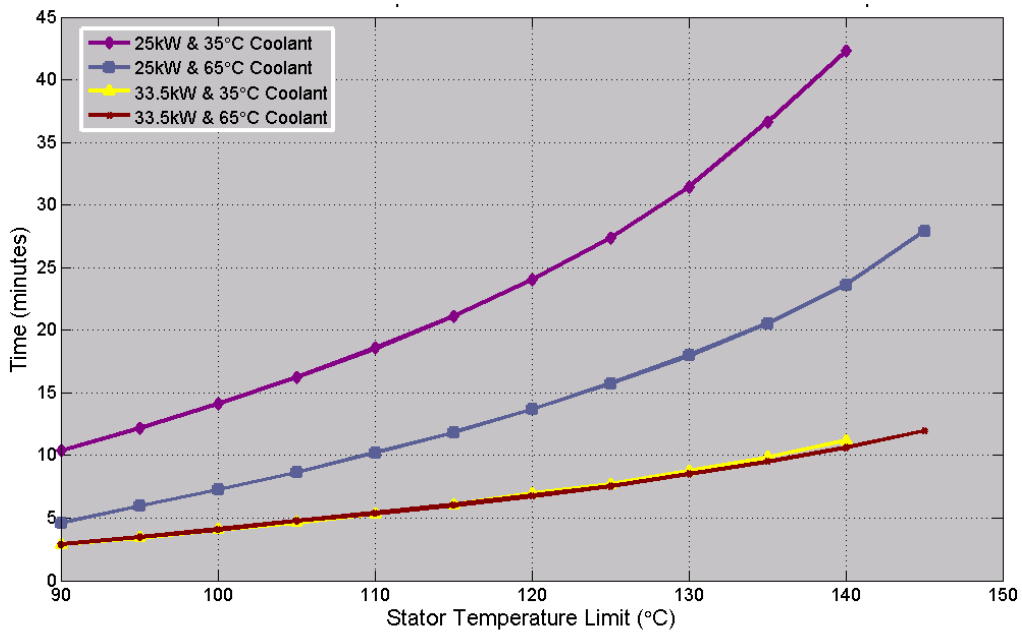

Fig. 3.35. Camry continuous duration at 3000 rpm with various power levels and coolant temperatures.

Characteristics similar to what are observed in Fig. 3.35 are observed in Fig. 3.36 where duration time is plotted versus stator temperature limit at 5000 rpm for various power and coolant temperature combinations. As the power level increases, the impact of coolant temperature upon duration decreases. For tests wherein thermal steady state was nearly reached, the curves approach a vertical asymptote which is located at the steady state stator temperature.

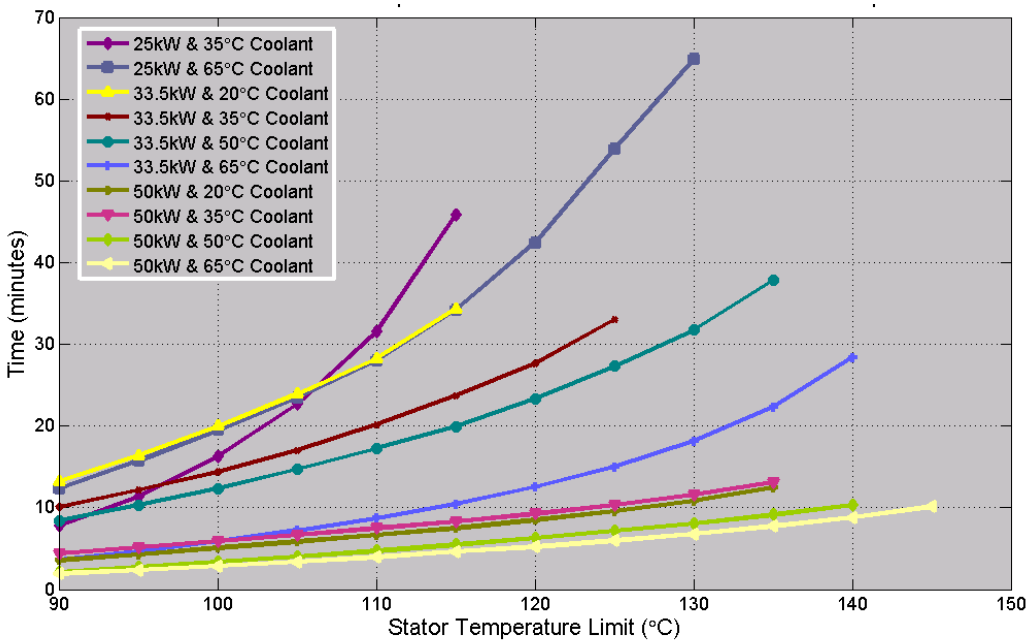

Fig. 3.36. Camry continuous duration at 5000 rpm with various power levels and coolant temperatures.

A graph of duration versus stator temperature limit at 7000 rpm with various power and coolant temperature combinations is shown in Fig. 3.37. Again, with increasing power, coolant temperature has a decreasing effect upon the duration of motor operation under these conditions. Note that all power-coolant temperature combinations and color correlations do not remain the same among Figs. 3.35, 3.36, and 3.37. A comparison of these figures indicates that coolant temperature has a greater impact upon the duration of operation at higher speeds. For example, the duration of operation is influenced more by coolant temperature at 7000 rpm and 25 kW than it is for 25 kW power levels at 3000 rpm and 5000 rpm.

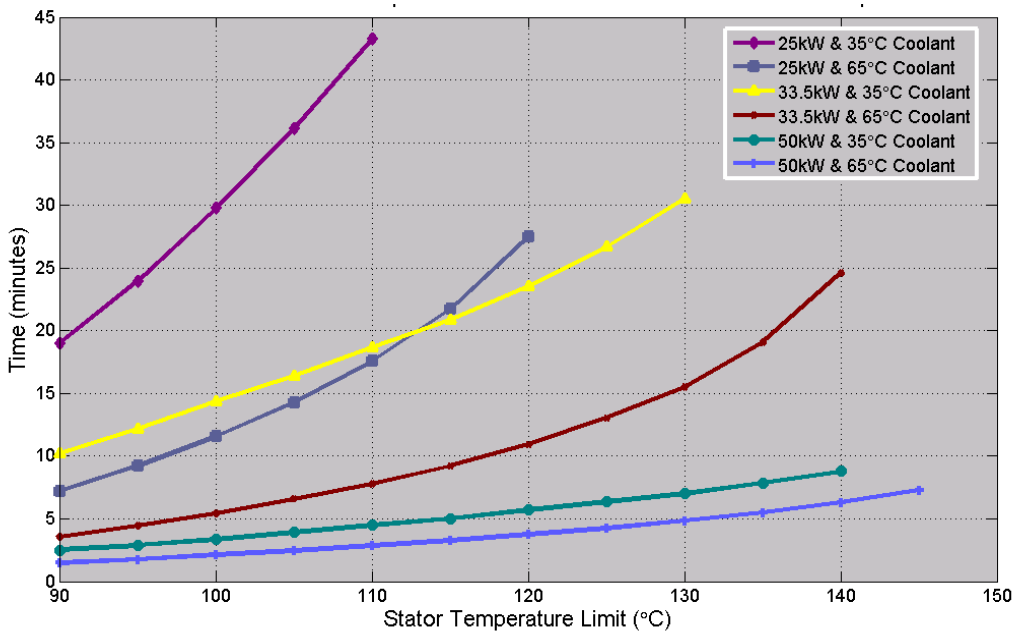

Fig. 3.37. Camry continuous duration at 7000 rpm with various power levels and coolant temperatures.

Note that in some of the tests in which lower coolant temperatures were used, the duration of operation was longer than that of a lower power level with a higher coolant level. This occurred because system temperatures were allowed to stabilize at each coolant temperature. For example, the duration of the 33.5 kW and 35ºC coolant temperature test condition is longer than that with the 25 kW and 65ºC coolant temperature test conditions if the stator temperature limitation is set at a low temperature. However, if the stator temperature limitation is set at a high level, the motor can operate longer at the 25 kW and 65ºC coolant temperature test condition. Thus, with 33.5 kW operation and a 35ºC coolant temperature, the entire system begins at a cooler temperature, yet the entire system temperature increases more quickly and eventually becomes hotter than if the system were operating at 25 kW operation with 65ºC, even though the system begins at a higher temperature (65ºC).

It is clear that defining the continuous operation capability of a motor depends on many variables, which even includes the definition of continuous operation. For example, continuous operation could be defined to be operation at a particular power level for an infinite amount of time, or a particular time restraint could be included in the definition. For some HEV applications, it is crucial that the motor is capable of operating continuously within particular power levels. For example, the Camry hybrid system requires torque from the motor and generator for the engine to supply power to the drive wheels. Many aspects must be considered for these conditions, and if properly designed, the volume and mass of the electric drive system can be optimized to match the demands of the system.

4. SUMMARY AND CONCLUSIONS

The 2007 Camry HEV subsystem assemblies were physically evaluated and comprehensively tested in the laboratory to fully assess their performance, efficiency, design, and packaging characteristics. The laboratory evaluations included back-emf, rotational loss, locked rotor, efficiency mapping, and extended-duration load tests. Overall, the Camry motor outperformed the Prius motor in terms of efficiency and equivalent torque and power, while the mass and volume of the system decreased significantly. Increased operation speed of the motor is the primary factor which provides the enhanced characteristics of the hybrid system. Additionally, the improved packaging and trench gate structure used in the PCU IGBTs led to a higher power density of the PCU components. The Camry inverter efficiencies are slightly lower than those of the Prius, yet the combined motor and inverter efficiencies of the Camry are still higher, especially for the low speed, high torque operation region. The lower motor efficiencies of the Prius have a much higher impact on the combined motor and inverter efficiencies than the impact of the slightly lower efficiencies of the Camry inverter.

Evaluations illustrate the benefits of moving to a high speed motor through improved packaging, higher efficiencies, increased performance, and improved continuous operation test results. Motor efficiencies are above 90% for a great portion of the operation range. Low speed efficiencies of the Camry are much higher than those of the Prius, which is particularly noticeable when the speed reduction gear ratio of 2.47 is applied to the efficiency map, and therefore the resulting torque is increased significantly. The peak power of the primary Camry motor is about 70 kW at 5000 rpm, which is much lower that the published rating of 105 kW. There are no specifications published for the generator and the published power rating may be for both the motor and generator. Simulations of this motor and a comparison of specific power characteristics with other high speed motors also suggest that the power rating is near 70 kW.

Continuous duration varies significantly with speed, specified stator temperature limit, and coolant temperature. A power level of 33.5 kW was maintained at 5000 rpm for about 30 minutes with 65°C coolant, at which a stator temperature of 140°C was reached. There is no standard for establishing continuous or peak power rating specifications for motors designed for HEV applications such as the hybrid Camry and Prius motors. For example, the Camry PMSM is able to sustain a power level of 50 kW at 5000 rpm for about 13 minutes with a stator temperature limit of 135ºC and coolant temperature of 35ºC; however, the duration is only about 8 minutes if a coolant temperature of 65ºC is applied. In addition to the unexpectedly low motor power rating, this highlights a very important reason for performing benchmarking tests on HEV subsystems – current technology must be verified objectively under consistent operating parameters before the results are used by the FCVT program and researchers. The influence of HEV specifications on technical goals and program planning would be drastically different if unclear published specifications of HEV systems were used as a baseline.

Among the vast amount of information obtained during benchmarking efforts, the significant findings are summarized in Table 4.1. Some of the information obtained from the Prius and Camry benchmarking studies has been and will be used by researchers to improve/verify analytical models. As a next step in the benchmarking efforts at ORNL, focus will be placed on an HEV system with improved power capabilities. These efforts are expected to be performed in FY2008 and will focus on the Lexus LS 600h hybrid subsystems, which are expected to include significant design improvements. Technological advances which facilitate higher power capability, power density, specific power, efficiency, and cost effectiveness of HEV components are essential as HEVs become increasingly dependant upon the electrical portion of the drive system and as the electric vehicle (EV) and HEV market continues to expand in the future.

Table 4.1. 2007 Camry/2004 Prius design comparison highlights

Parameter	Camry	Prius	Comments
Transaxle			
Motor power rating.	70 kW	50 kW	Published Camry power rating is likely a combination of motor and generator ratings.
Motor lamination stack length.	6.07 cm (2.39″)	8.40 cm (3.3″)	Reduced by 2.33 cm (0.91″).
Motor mass.	41.7 kg	45.0 kg	7.3% reduction.
Motor volume.	14.8 L	15.4 L	3.9% reduction.
Motor specific power.	1.68 kW/kg	1.11 kW/kg	Improved by a factor of 1.5.
Motor power density.	4.73 kW/L	3.25 kW/L	Improved by a factor of 1.5.
Equivalent torque rating.	667 Nm	400 Nm	Camry torque value from speed reduction gear (short duration).
Motor speed rating.	14,000 rpm	6,000 rpm	
Motor winding configuration.	Parallel	Series	
Power split.			
PCU			
Nominal battery voltage.	244.8 V	201.6 V	Up to 20% higher during operation.
Maximum dc-link voltage.	650 Vdc	500Vdc	
Boost converter power rating.	30 kW	20 kW	
Filter capacitor (battery level).	500 Vdc, 378 μF	600 Vdc, 282 μF	
Smoothing capacitor (boosted level).	750 Vdc, 2098 μF	600 Vdc, 1,130 μF	
Entire PCU mass.	17.86 kg	21.2 kg	15.8% reduction.
Entire PCU volume.	11.7 L	17.8 L	Prius PCU includes 12V dc-dc and compressor inverter, Camry PCU does not.
Motor inverter mass.	7.5 kg	8.8 kg	14.7% reduction.
Motor inverter volume.	~6 L	8.7 L	31% reduction.
Motor inverter specific power.	9.3 kW/kg	5.7 kW/kg	Improved by a factor of 1.6.
Motor inverter power density.	11.7 kW/L	5.7 kW/L	Improved by a factor of 2.1.
Boost converter mass.	6.6 kg	4.8 kg	37.5% increase.
Boost converter volume.	3.5 L	5.1 L	31.3% reduction.
Boost converter specific power.	4.5 kW/ kg	4.2 kW/kg	Improved by 7%.
Boost converter power density.	8.6 kW/L	3.9 kW/L	Improved by a factor of 2.21.

REFERENCES

1. Source: http://www.eere.energy.gov/vehiclesandfuels/technologies/systems/index.shtml.

2. J. S. Hsu, S. C. Nelson, P. A. Jallouk, C. W. Ayers, R. H. Wiles, S. L. Campbell, C. L. Coomer, K. T. Lowe, and T. A. Burress, *Report on Toyota Prius Motor Thermal Management*, ORNL/TM-2005/33, UT-Battelle, LLC, Oak Ridge National Laboratory, Oak Ridge, Tennessee, February 2005.

3. R. H. Staunton, C. W. Ayers, J. Chiasson, T. A. Burress, and L. D. Marlino, *Evaluation of 2004 Toyota Prius Hybrid Electric Drive System,* ORNL/TM-2006-423, UT-Battelle, LLC, Oak Ridge National Laboratory, Oak Ridge, Tennessee, May 16, 2006.

4. R. H. Staunton, T. A. Burress, and L. D. Marlino, *Evaluation of 2005 Honda Accord Hybrid Electric Drive System,* ORNL/TM-2006-535, UT-Battelle, LLC, Oak Ridge National Laboratory, Oak Ridge, Tennessee, September 2006.

5. *Camry Hybrid Vehicle New Car Features 2007*, Toyota Motor Corporation, March 2006.

APPENDIX A: 2004 PRIUS POWER CONVERTER UNIT PACKAGING ASSESSMENTS

2004 Prius Motor Inverter Mass and Volume Assessment

Total Volume of PCU casing is **17.8 L** as depicted in Fig. A.1.

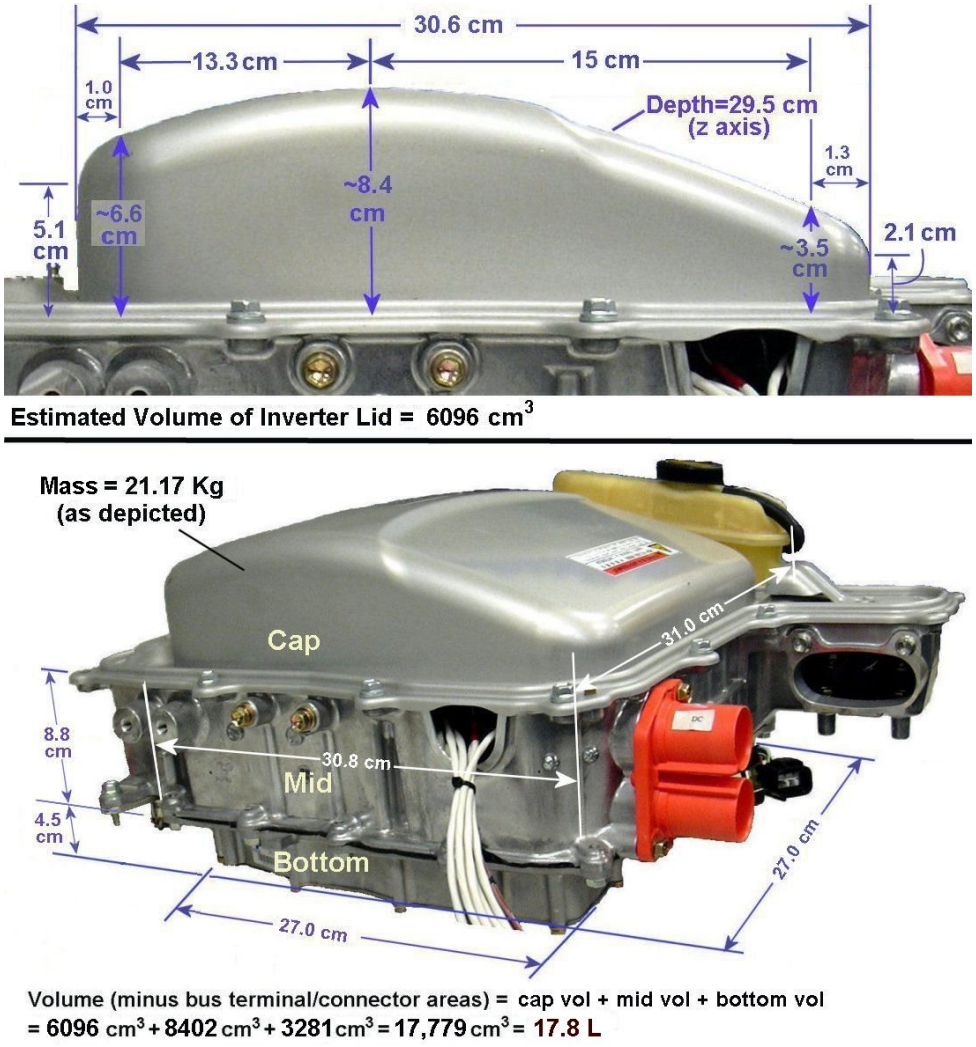

Fig. A.1. Volume of entire Prius PCU assembly.

Total volume of "inverter *only"* is **8.7 L** and is derived as follows:

- Mid section volume is reduced by 55% after the exclusion of the volume associated with the converter components, the generator portion of the inverter board (a 1/2 reduction), the generator portion of the power module (a 1/3 reduction) and the corresponding portion of the cold plate (a 60% reduction). See Fig. A.2 as an aid in visualization.

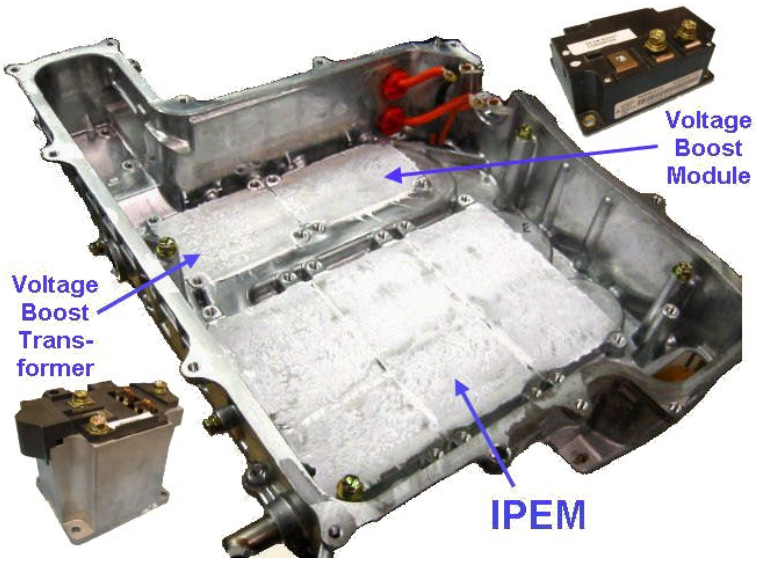

Fig. A.2. Empty inverter/converter housing showing cold plate surfaces.

- It is also reduced by the deletion of the bottom compartment (unrelated circuitry).
- The lid and capacitor volume, although not optimized, is scaled by a factor of 1130 μF/(282 μF + 1130 μF) = 4/5 to account for the separation of the boost converter and inverter capacitors.

Total mass of PCU casing as depicted in Fig. A.1 is **21.2 kg**.
Total mass of "inverter *only*" is **8.8 kg** and is derived in a similar manner that volume was derived (80% of capacitor mass, 45% of mid-section mass, and 0% of bottom section mass). The reduction of mid-section mass is actually more severe than the "45%" suggests since the high-mass converter transformer and converter power module were first fully excluded.

2004 Prius Bi-Directional Boost Converter Mass and Volume Assessment

The general circuit diagram for the converter is shown in Fig. A.3, showing that the converter topology is that of a conventional bidirectional boost converter. The figure also supplies mass and volume figures of the inductor and IPM.

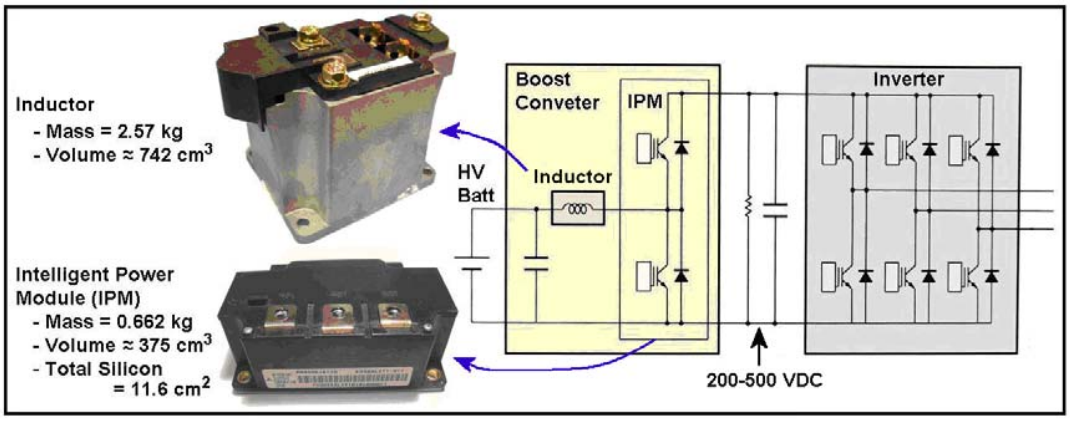

Fig. A.3. General circuit schematic of the Prius inverter.

During periods of maximum power demand from the driver, the converter provides up to ~20 kW to the inverter/motor system and the vehicle generator supplies up to ~30 kW. This power split allows a reduction in size of the high-cost HV battery and the converter, while the extent of fully electric operation is compromised.

Excluding the cold plate, the volume and mass totals for the ~20 kW boost converter IPM and inductor are ~1.12 L and 3.23 kg, respectively.

Volume calculation approach A: The volume of the cold plate under the 2 converter components (including adjacent mounting holes) is 19 mm × 100 mm × 250 mm = 0.48 L. However, this approach ignores the space enclosed by the converter portion of the casing.

Volume calculation approach B: It is more pertinent to consider the entire volume that includes the cold plate, items mounted on it, and surrounding space enclosed in the casing. This volume is 335 mm × 100 mm × 140 mm = 4.7 L.

It is estimated that 15% of the casing mass is dedicated to the bidirectional converter. Since the casing shell is 6.45 kg, the mass reduction is ~1 kg.

Capcitor: The entire capacitor volume is 1.8 L. The volume associated with the boost converter is approximately 1.8 × 282 μF/(282 μF + 1130 μF) = 1.8/5 = 0.36 L. The capacitor mass is approximately 2.79 kg /5 = 0.56 kg.

Conclusions: Accounting for the inductor, IPM, casing, and capacitor the converter system volume is **5.1 L** and the mass is **4.8 kg**.

APPENDIX B: PRIUS AND CAMRY CAPACITOR TEST RESULTS

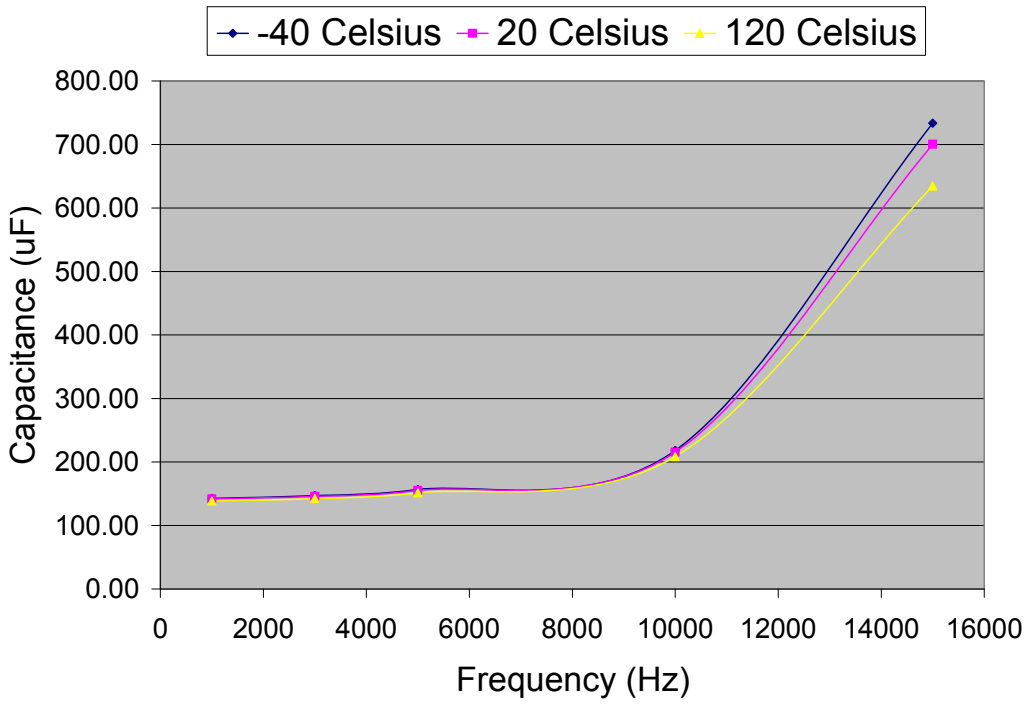

Fig. B.1. Prius single 141 µF capacitor from 1,130 µF module, capacitance vs. frequency.

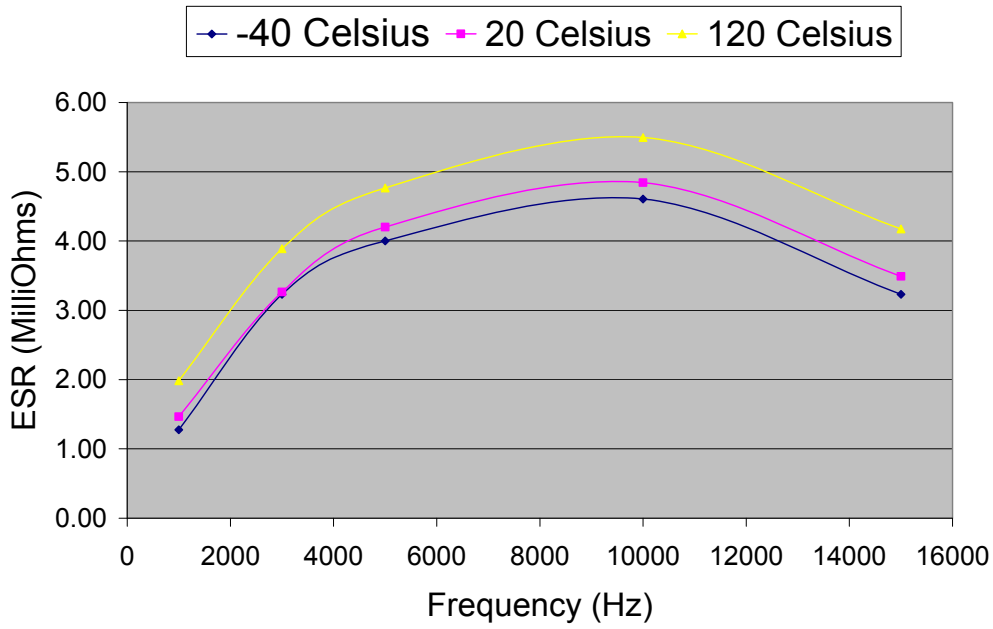

Fig. B.2. Prius single 141 µF capacitor from 1,130 µF module, ESR vs. frequency.

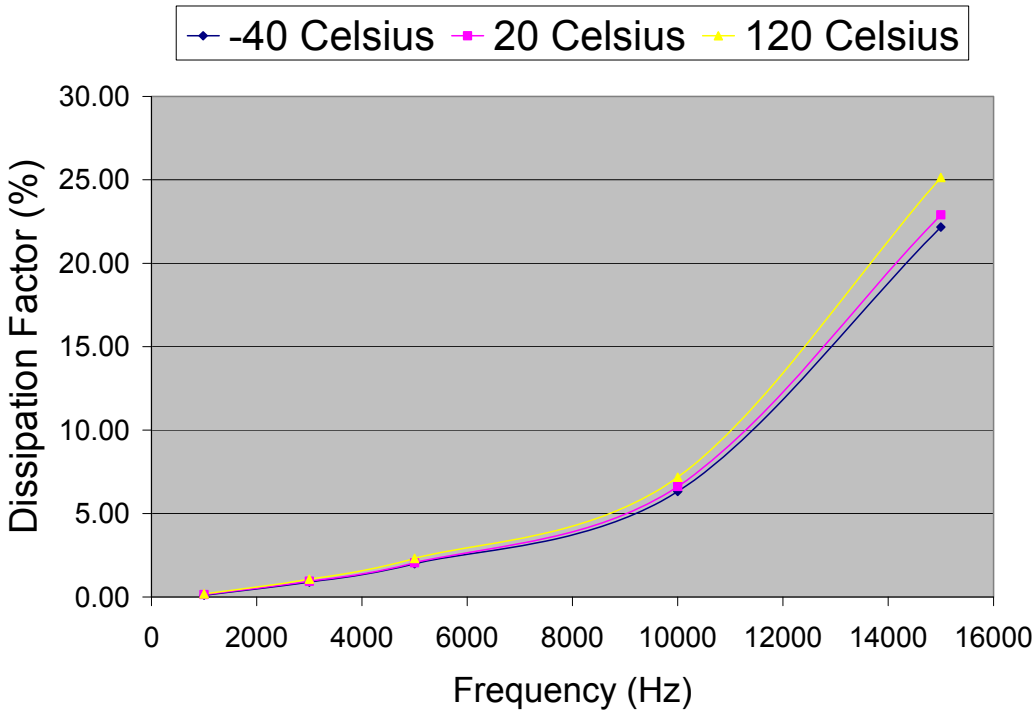

Fig. B.3. Prius single 141 µF capacitor from 1,130 µF module, DF vs. frequency.

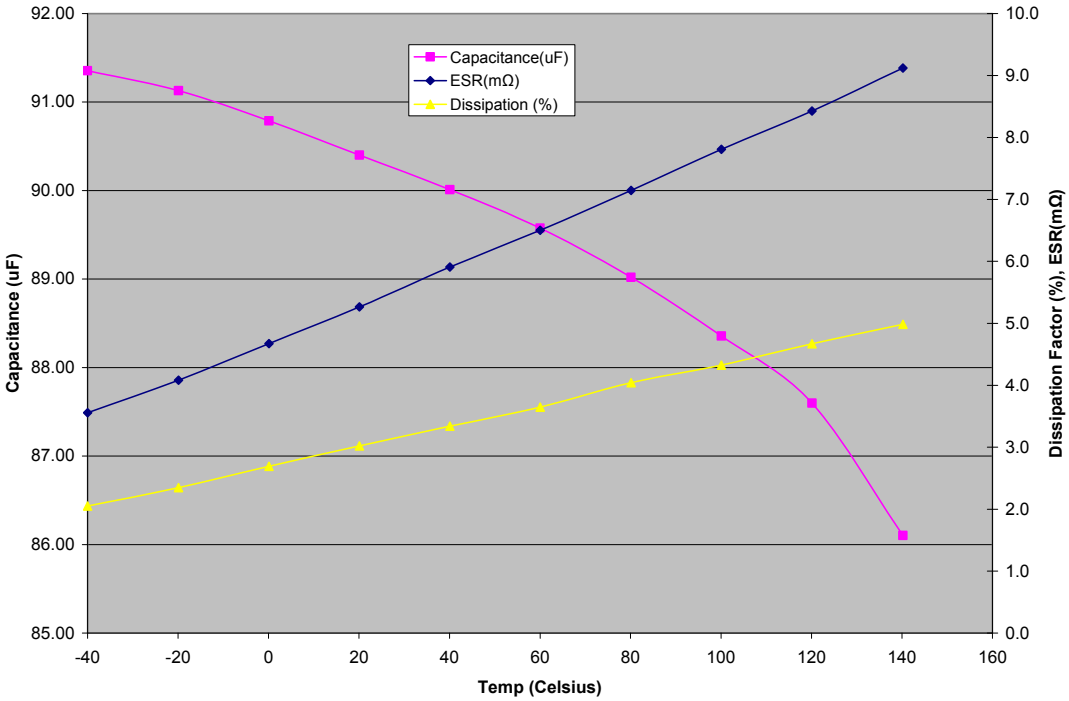

Fig. B.4. Camry single 86 µF capacitor, capacitance, ESR, and DF vs. temperature at 10 kHz.

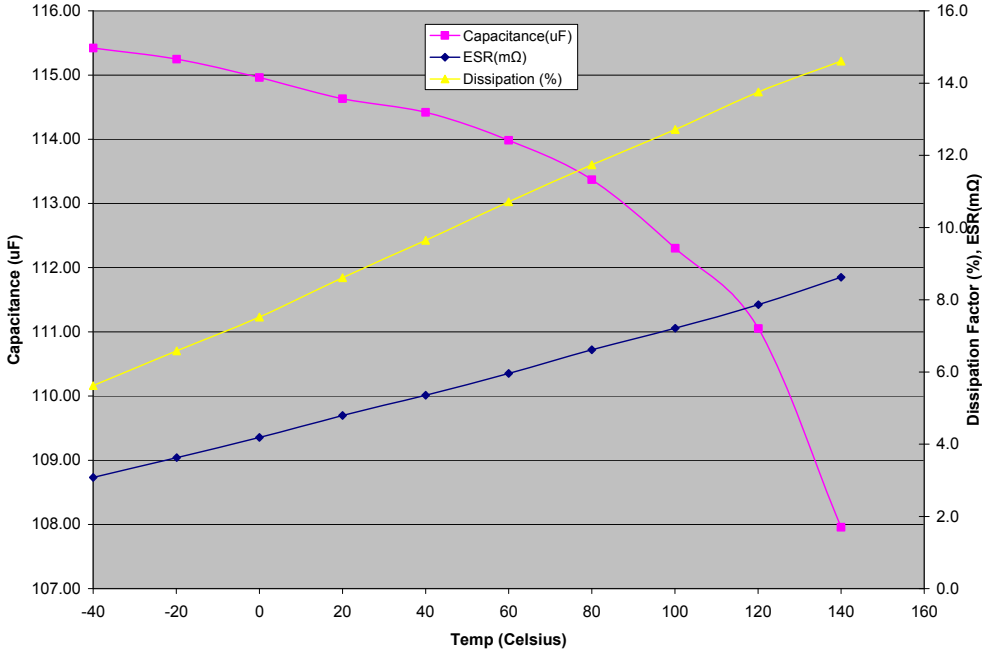

Fig. B.5. Camry single 86 µF capacitor, capacitance, ESR, and DF vs. temperature at 25 kHz.

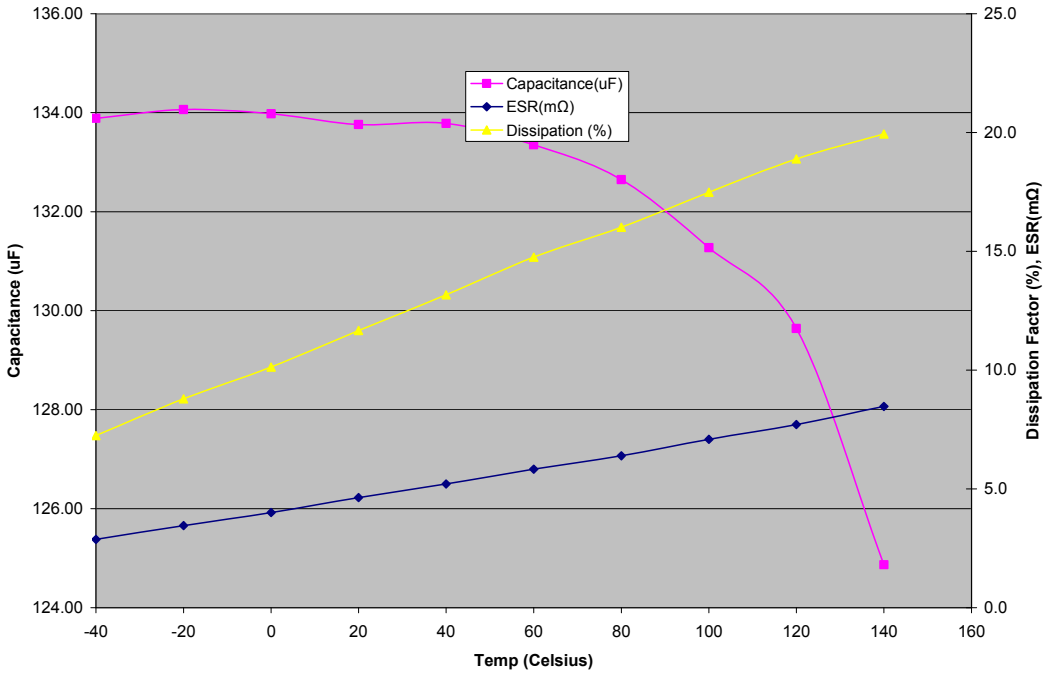

Fig. B.6. Camry single 86 µF capacitor, capacitance, ESR, and DF vs. temperature at 30 kHz.

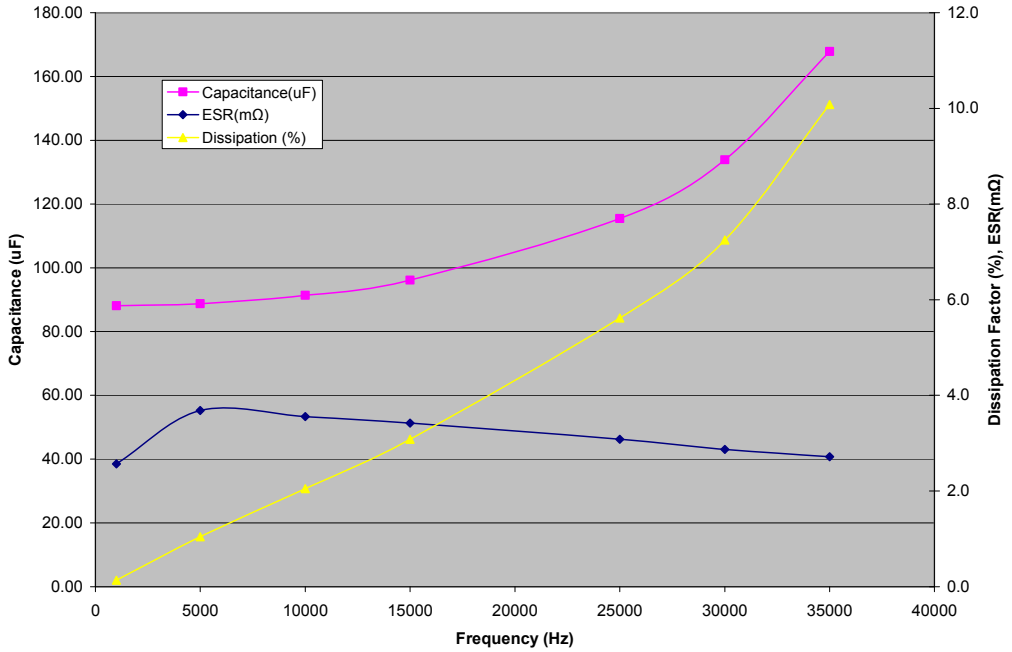

Fig. B.7. Camry single 86 µF capacitor, capacitance, ESR, and DF vs. frequency at -40ºC.

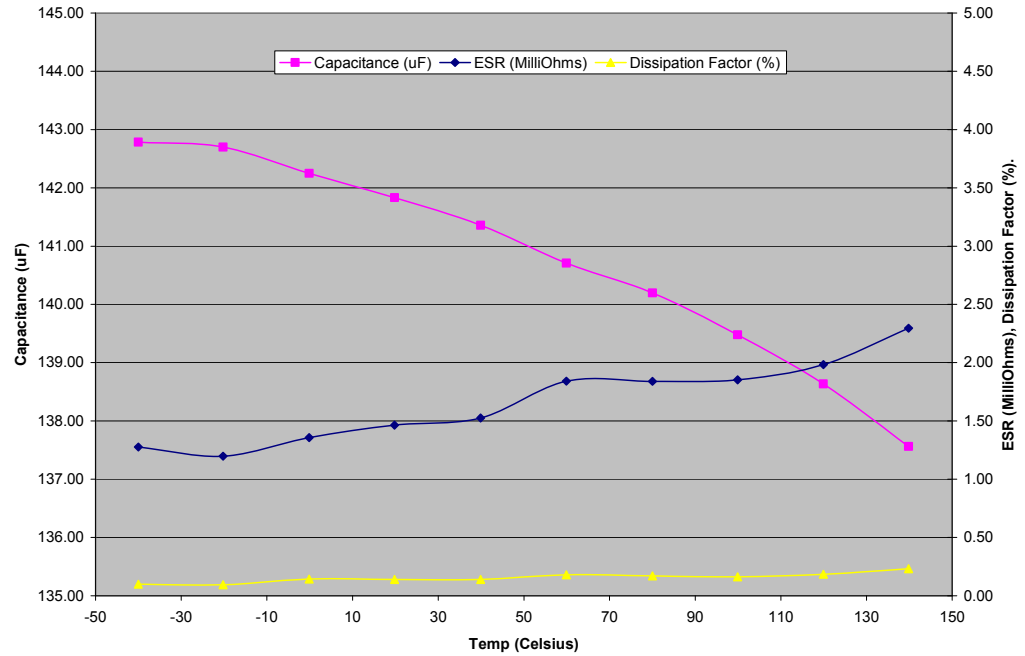

Fig. B.8. Prius single 141 µF capacitor, capacitance, ESR, and DF vs. temperature at 1 kHz.

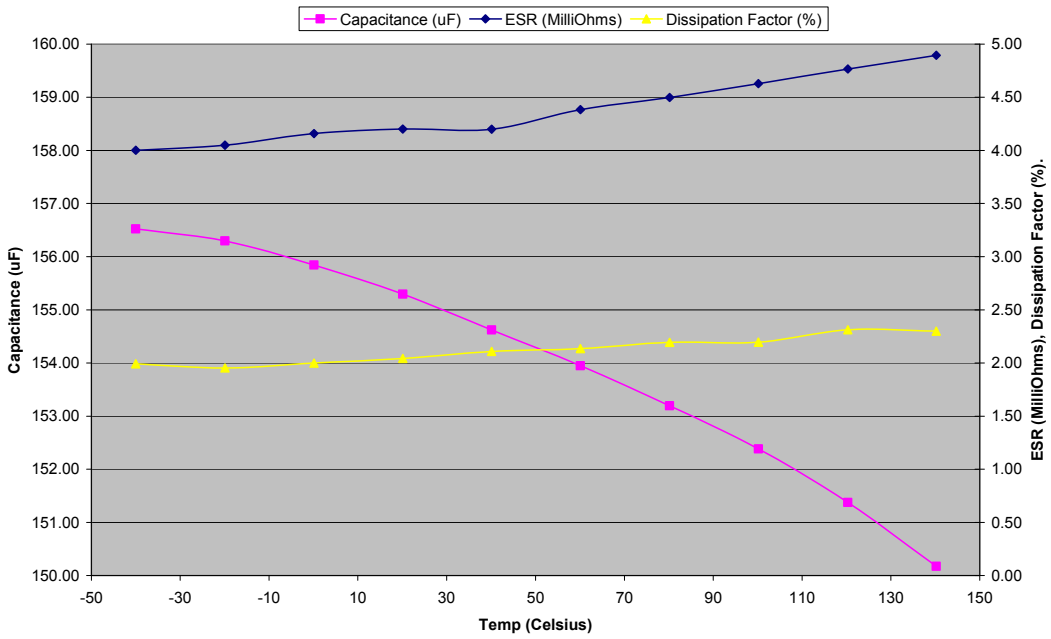

Fig. B.9. Prius single 141 µF capacitor, capacitance, ESR, and DF vs. temperature at 5 kHz.

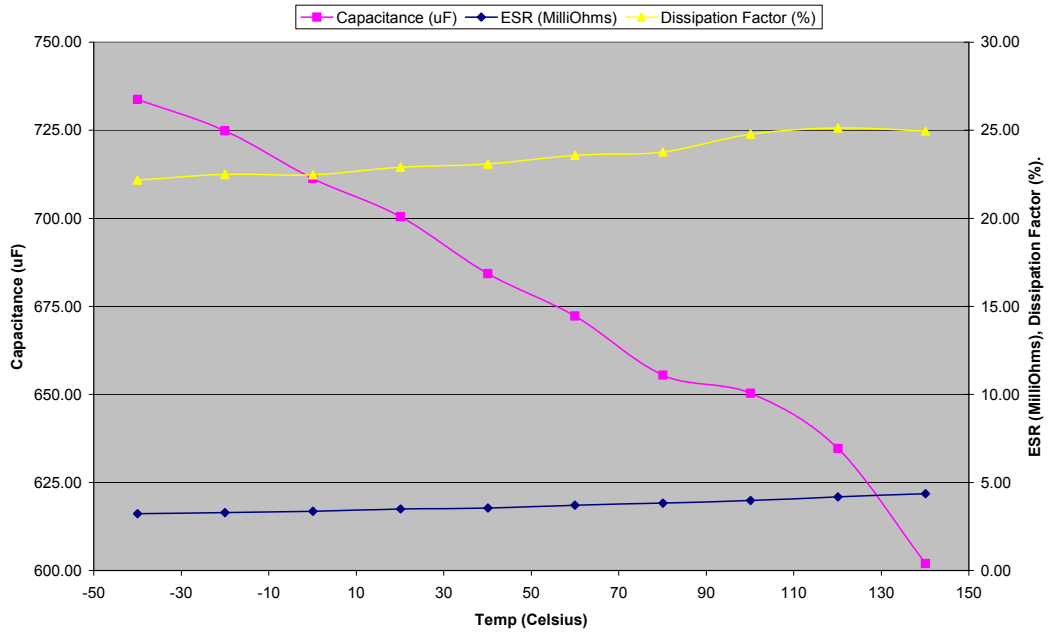

Fig. B.10. Prius single 141 µF capacitor, capacitance, ESR, and DF vs. temperature at 15 kHz.

APPENDIX C: 2004 PRIUS TRANSAXLE PACKAGING ASSESSMENTS

2004 Prius Motor Mass and Volume Assessment

The configuration of the motor rotor and stator are shown in Fig. C.1.

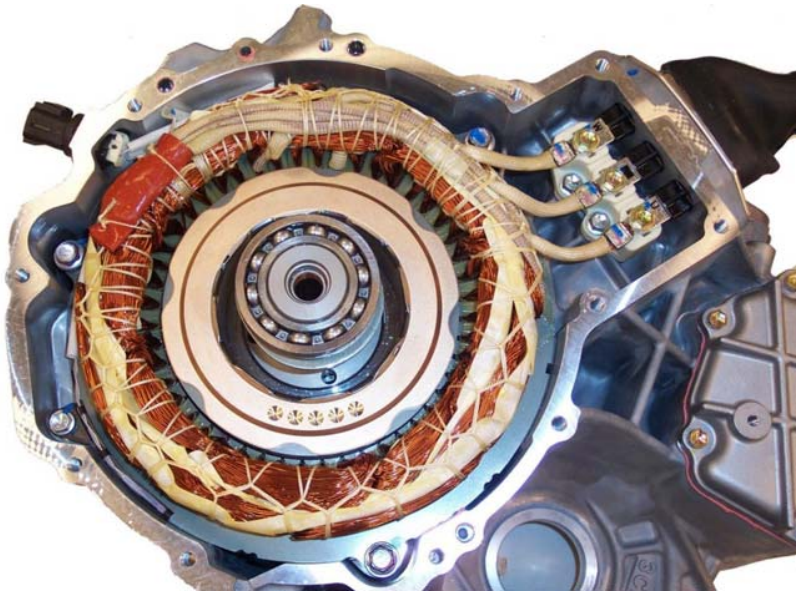

Fig. C.1. 2004 Prius motor rotor and stator.

Figure C.1 shows three views of the PMSM housing with selected dimensions called out. As indicated, about 3/4th of the casing houses the PMSM rotor and stator and the remainder encloses part of the gearbox. The portion of the casing that houses the PMSM is roughly cylindrical and that is the geometry used for the purposes of estimating the PMSM casing volume. Based on the average of 3 measurements of casing diameter, the cylinder diameter can be assumed to be ~29.9 cm. The depth of the PMSM housing extending from the end plate to the surface identified in the upper left photo in Fig. C.2 is 20.5 cm. This results in a volume of 14,400 cm^3 excluding the three-phase terminal block housing and the cooling passages that protrude from the surface of the casing. Including all 3 volumes results in a total of 15,400 cm^3 (15.4 L). This volume and the 50 kW peak power specification result in a peak power density of 3.25 kW/L.

The mass of the PMSM was determined in order to estimate the specific power. The masses of the components of the Prius PMSM are:

Stator:	25.9 kg
Rotor:	10.2 kg
Case:	6.36 kg (machined – see below)
Case cover:	2.49 kg
Total mass of motor:	**44.95 kg**

The casing for the PMSM has (1) a portion that encloses one end of the gear box, and (2) compartments that enclose the gear-shift-lever-to-shift-plunger linkages. These areas are unrelated to the PMSM and were therefore machined off of the structure to obtain a new 6.36 kg mass (the original casing mass was 13.9 kg). The resulting specific power for the PMSM is 1.11 kW/kg.

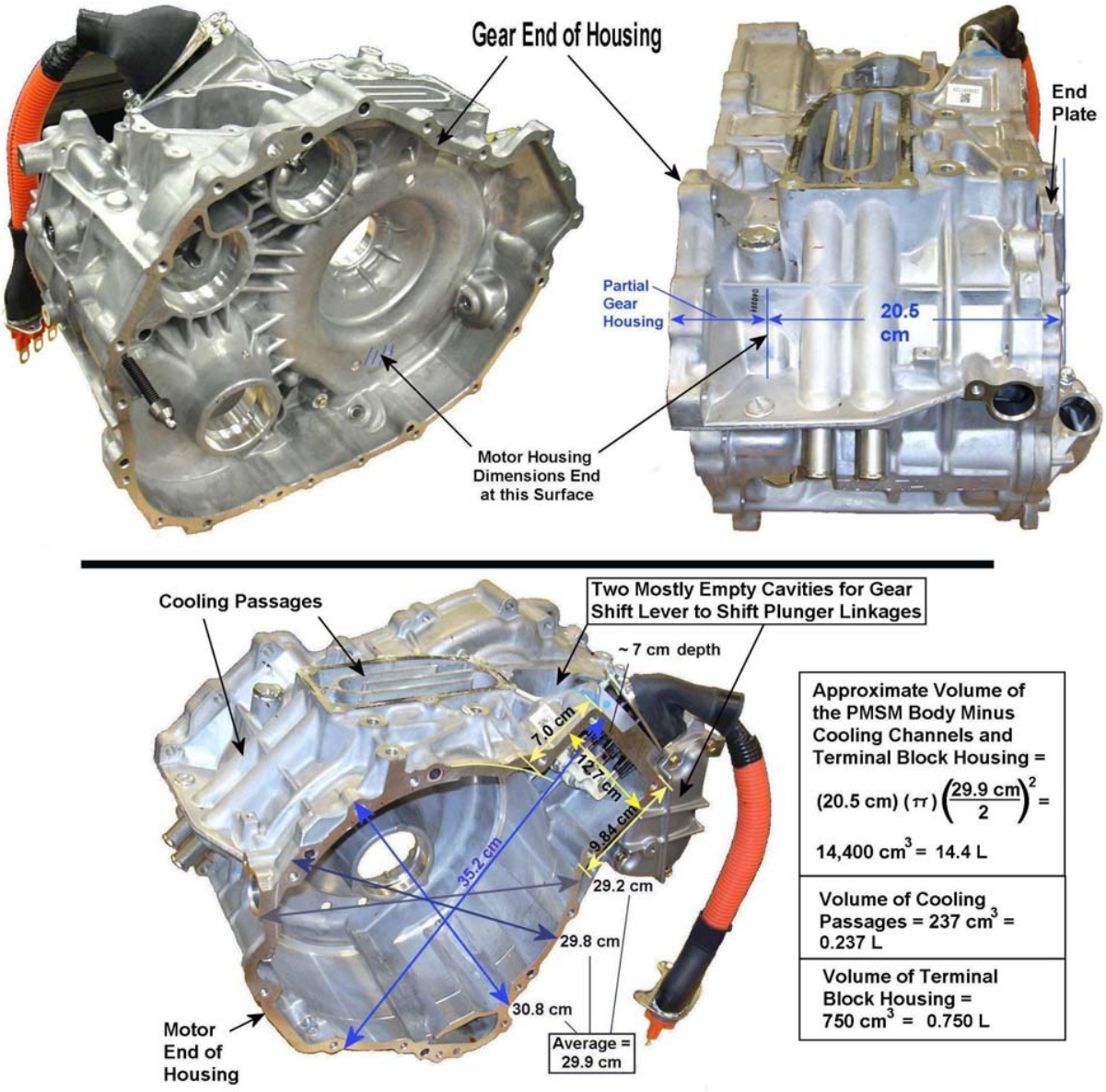

Fig. C.2. Casing of the 2004 Prius PMSM with dimensions and volume calculations.

DISTRIBUTION

Internal

1. D. J. Adams
2. T. A. Burress
3. S. L. Campbell
4. C. L. Coomer
5. J. P. Cunningham
6. E. C. Fox
7. K. P. Gambrell
8. J. S. Hsu
9. L. D. Marlino
10. M. Olszewski
11. L. E. Seiber
12. R. H. Staunton
13. Laboratory Records

External

14. F. D. Barlow III, University of Idaho, Department of Electrical & Computer Engineering, Buchanan Engineering Laboratory, Rm. 211, 607 Urquhart Avenue, Moscow, ID 83844-1023, fbarlow@uidaho.edu.
15. R. Al-Attar, DCX, raa9@dcx.com.
16. S. J. Boyd, U.S. Department of Energy, EE-2G/Forrestal Building, 1000 Independence Avenue, S.W., Washington, D.C. 20585.
17. T. Q. Duong, U.S. Department of Energy, EE-2G/Forrestal Building, 1000 Independence Avenue, S.W., Washington, D.C. 20585.
18. R. R. Fessler, BIZTEK Consulting, Inc., 820 Roslyn Place, Evanston, Illinois 60201-1724.
19. G. Hagey, Sentech, Inc., 501 Randolph St., Williamsburg, Virginia 23185.
20. E. Jih, Ford Motor Company, Scientific Research Laboratory, 2101 Village Road, MD-1170, Rm. 2331, Dearborn, Michigan 48121.
21. K. J. Kelly, National Renewable Energy Laboratory, 1617 Cole Boulevard, Golden, Colorado 80401.
22. A. Lee, Daimler Chrysler, CIMS 484-08-06, 800 Chrysler Drive, Auburn Hills, Michigan 48326-2757.
23. F. Leonardi, Ford Motor Company, 15050 Commerce Drive, North, Dearborn, Michigan 48120-1261.
24. F. Liang, Ford Motor Company, Scientific Research Laboratory, 2101 Village Road, MD1170, Rm. 2331/SRL, Dearborn, Michigan 48121.
25. M. W. Lloyd, Energetics, Inc., 7164 Columbia Gateway Drive, Columbia, Maryland 21046.
26. J. Maquire, General Motors Advanced Technology Center, 3050 Lomita Boulevard, Torrance, California 90505.
27. M. Mehall, Ford Motor Company, Scientific Research Laboratory, 2101 Village Road, MD-2247, Rm. 3317, Dearborn, Michigan 48124-2053.
28. J. A. Montemarano, Naval Surface Warfare Center, Carderock Division; Code 642, NSWD, 9500 MacArthur Boulevard; West Bethesday, Maryland 20817.
29. N. Olds, United States Council for Automotive Research (USCAR), nolds@uscar.org
30. S. A. Rogers, U.S. Department of Energy, EE-2G/Forrestal Building, 1000 Independence Avenue, S.W., Washington, D.C. 20585.
31. G. S. Smith, General Motors Advanced Technology Center, 3050 Lomita Boulevard, Torrance, California 90505.
32. E. J. Wall, U.S. Department of Energy, EE-2G/Forrestal Building, 1000 Independence Avenue, S.W., Washington, D.C. 20585.
33. B. Welchko, General Motors Advanced Technology Center, 3050 Lomita Boulevard, Torrance, California 90505.
34. P. G. Yoshida, U.S. Department of Energy, EE-2G/Forrestal Building, 1000 Independence Avenue, S.W., Washington, D.C. 20585.